

The $Z\gamma$ and diphoton decays of the Higgs boson as a joint probe of low energy SUSY models

Junjie Cao^{1,2}, Lei Wu³, Peiwen Wu³, Jin Min Yang³

¹ *Department of Physics, Henan Normal University, Xinxiang 453007, China*

² *Center for High Energy Physics, Peking University, Beijing 100871, China*

³ *State Key Laboratory of Theoretical Physics,
Institute of Theoretical Physics, Academia Sinica, Beijing 100190, China*

Abstract

In light of recent remarkable progress in Higgs search at the LHC, we study the rare decay process $h \rightarrow Z\gamma$ and show its correlation with the decay $h \rightarrow \gamma\gamma$ in low energy SUSY models such as CMSSM, MSSM, NMSSM and nMSSM. Under various experimental constraints, we scan the parameter space of each model, and present in the allowed parameter space the SUSY predictions on the $Z\gamma$ and $\gamma\gamma$ signal rates in the Higgs production at the LHC and future e^+e^- linear colliders. We have following observations: (i) Compared with the SM prediction, the $Z\gamma$ and $\gamma\gamma$ signal rates in the CMSSM are both slightly suppressed; (ii) In the MSSM, both the $Z\gamma$ and $\gamma\gamma$ rates can be either enhanced or suppressed, and in optimal case, the enhancement factors at the LHC can reach 1.1 and 2 respectively; (iii) In the NMSSM, the $Z\gamma$ and $\gamma\gamma$ signal rates normalized by their SM predictions are strongly correlated, and at the LHC the rates vary from 0.2 to 2; (iv) In the nMSSM, the $Z\gamma$ and $\gamma\gamma$ rates are both greatly reduced. Since the correlation behavior between the $Z\gamma$ signal and the $\gamma\gamma$ signal is so model-dependent, it may be used to distinguish the models in future experiments.

PACS numbers: 14.80.Da,14.80.Ly,12.60.Jv

I. INTRODUCTION

Based on the measurements of $\gamma\gamma$ and ZZ^* channels the ATLAS and CMS collaborations have independently provided compelling evidence for a bosonic resonance around 125-126 GeV [1, 2]. This is a great triumph for particle physics, but it also leads to a host of new questions about the nature of the boson. So far there exist large uncertainties in determining the rates of the two channels, and meanwhile, observation of the boson through other signals such as $b\bar{b}$ and $\tau^+\tau^-$ channels is still far away from becoming significant[3]. So although the preliminary data of the LHC indicate that the boson closely resembles the Higgs boson in the Standard Model (SM), the deficiencies of the SM itself such as gauge hierarchy problem suggest new physics explanation of the boson. Obviously, in order to decide the right underlying theory, the LHC should exhaust its potential to measure the decay channels of the boson as accurately as possible in its high luminosity phase.

Among the decay modes of the Higgs-like boson h , the diphoton channel plays a very important role in determining its mass, spin and parity[4]. At the same time, since the diphoton channel is mediated by loops of charged particles, it also acts as a sensitive probe to new physics. In fact, this feature has been widely utilized to explain the results of the ATLAS and CMS collaborations on the inclusive diphoton signal in 2012[5–14], which were 1.9 ± 0.5 and 1.56 ± 0.43 respectively for the signal rate normalized by its SM prediction [1, 2]. In this note, we concentrate on another decay mode $h \rightarrow Z\gamma$. In the SM, the branching ratio of this decay is about two thirds of that for the diphoton decay, and just like the diphoton signal, it can provide a clean final-state topology in determining the properties of the boson, such as its mass, spin and parity[15]. Moreover, since new charged particles affecting the diphoton decay can also contribute to the $Z\gamma$ decay, the two decay modes should be correlated, and therefore studying them in a joint way can reveal more details about the underlying physics. Albeit the advantages, in contrast to the diphoton decay which has been intensively studied, the $Z\gamma$ decay was paid little attention in the past. For example, since the discovery of the boson only several works have been devoted to this decay in new physics models such as the type-II seesaw model[16], the Georgi-Machacek model[17], the extensions of the SM by charged scalars in different $SU(2)_L$ representations[18] and the SM with extra colored scalars[19], and until very recently have the CMS and ATLAS collaborations set an upper limit on the ratio $\sigma_{Z\gamma}/\sigma_{Z\gamma}^{\text{SM}} < 10$ [20]. Note that although the $Z\gamma$ signal suffers

from a large irreducible background at the LHC [20], the Higgs event from the process $e^+e^- \rightarrow Zh \rightarrow ZZ\gamma$ can be easily reconstructed at the next generation linear collider with the center of mass energy around 250 GeV [21], which is very helpful in suppressing the background for such a signal. So there is a good prospect to precisely measure this decay in the future.

In the following, we focus on the $Z\gamma$ decay channel of the SM-like Higgs boson h in low energy supersymmetric models such as the Constrained Minimal Supersymmetric Standard Model (CMSSM)[22], the Minimal Supersymmetric Standard Model (MSSM)[23, 24], the Next-to-Minimal Supersymmetric Standard Model (NMSSM)[25] and the Nearly Minimal Supersymmetric Standard Model (nMSSM)[26]. We investigate the $Z\gamma$ signal of the Higgs production at the LHC and future e^+e^- linear colliders, and especially, we study its correlations with the $\gamma\gamma$ signal. As we will show below, the $Z\gamma$ signal rate may be either enhanced or suppressed in SUSY, and its correlation behavior is so model-dependent that it may be utilized to distinguish the models in high luminosity phase of the LHC.

This work is organized as follows. In Section II we introduce the basic features of the SUSY models and present some formulae relevant to our calculation. In Section III we first discuss the effects of new charged SUSY particles on the partial decay widths of $h \rightarrow Z\gamma$, then we study in a comparative way the $Z\gamma$ and $\gamma\gamma$ signal rates of the Higgs production at different colliders. Finally, we draw the conclusions in Section IV. Various couplings used in the calculation are given in the Appendix.

II. THE MODELS AND ANALYTIC FORMULAE

In a low energy supersymmetric gauge theory, the explicit form of its Lagrangian is determined by the gauge symmetry, superpotential and also soft breaking terms. As for the four models considered in this work, their differences mainly come from the superpotential, which is the source for the Yukawa interactions of fermions and self interactions of scalars.

MSSM and CMSSM : The MSSM[23, 24] contain two Higgs doublets H_u, H_d and it predict five physical Higgs bosons, of which two are CP-even, one is CP-odd and two are charged. Its superpotential takes following form

$$W^{\text{MSSM}} = W_F + \mu \hat{H}_u \cdot \hat{H}_d, \quad (1)$$

where W_F denotes the Yukawa interaction, and its form is given by

$$W_F = \bar{u}Y_u\hat{Q} \cdot \hat{H}_u - \bar{d}Y_d\hat{Q} \cdot \hat{H}_d - \bar{e}Y_e\hat{L} \cdot \hat{H}_d. \quad (2)$$

After considering appropriate soft breaking terms, one can write down the Higgs potential as

$$\begin{aligned} V^{\text{MSSM}} = & (|\mu|^2 + m_{H_u}^2)|H_u^0|^2 + (|\mu|^2 + m_{H_d}^2)|H_d^0|^2 \\ & - (B\mu H_u^0 H_d^0 + \text{h.c.}) + \frac{1}{8}(g_2^2 + g_1^2)(|H_u^0|^2 - |H_d^0|^2)^2, \end{aligned} \quad (3)$$

where m_{H_u} , m_{H_d} and B are all soft parameters with mass dimension, terms proportional to $|\mu|^2$ come from the F -term of the superpotential, and the last term comes from gauge symmetry (so called D -term). This potential indicates that, after the electroweak symmetry breaking, the μ -parameter is related to the Higgs vacuum expectation value (vev) and so it should be $\mathcal{O}(100\text{GeV})$. But on the other hand, since μ as the only parameter with mass dimension appears in the superpotential, its value should naturally take SUSY-preserving scale. Such a tremendously large scale gap is usually referred as the μ -problem [27].

The theoretical framework of the CMSSM[22] is exactly same as that of the MSSM, and the only difference between them comes from the fact that in the general MSSM, all soft breaking parameters are independent[28], while in the CMSSM they are correlated. Explicitly speaking, the CMSSM assumes following universal soft breaking parameters at SUSY breaking scale (usually chosen at the Grand Unification scale)[29]

$$M_{1/2}, M_0, A_0, \tan\beta, \text{sign}(\mu), \quad (4)$$

with $M_{1/2}$, M_0 and A_0 denoting gaugino mass, scalar mass and trilinear interaction coefficient respectively, and evolves the four parameters down to weak scale to get all the soft breaking parameters of the MSSM. In this sense, the parameter space of the CMSSM should be considered as a subset of that for the MSSM, and so is its phenomenology.

NMSSM and nMSSM : In order to solve the μ -problem in the MSSM, various singlet extensions of the MSSM were proposed in history, and among them the most well known models include the NMSSM and the nMSSM. The superpotentials of these two models are respectively given by [26, 30]

$$W^{\text{NMSSM}} = W_F + \lambda\hat{S}\hat{H}_u \cdot \hat{H}_d + \frac{\kappa}{3}\hat{S}^3, \quad (5)$$

$$W^{\text{nMSSM}} = W_F + \lambda\hat{S}\hat{H}_u \cdot \hat{H}_d + \xi_F M_n^2 \hat{S}, \quad (6)$$

where λ , κ and ξ_F are dimensionless parameters of order 1, and the dimensionful parameter M_n may be naturally fixed at weak scale in certain basic frameworks where the parameter is generated at a high loop level[30]. One attractive feature of both the models comes from the fact that, after the real scalar component of \hat{S} develops a vev $\langle S \rangle$, an effective μ parameter is generated by $\mu_{\text{eff}} = \lambda \langle S \rangle$, and its value may be as low as about 100GeV without conflicting with current experiments [12] (in contrast, the μ parameter in the MSSM must be larger than about 200GeV[12]). Another attractive feature of the models is that the Z boson mass may be obtained with less fine tuning than the MSSM[31]. In the SUSY models, after the minimization of the Higgs potential, the Z boson mass is given by[31]

$$\frac{M_Z^2}{2} = \frac{(m_{H_d}^2 + \Sigma_d) - (m_{H_u}^2 + \Sigma_u) \tan^2 \beta}{\tan^2 \beta - 1} - \mu^2, \quad (7)$$

where $m_{H_d}^2$ and $m_{H_u}^2$ represent the soft SUSY breaking masses of the Higgs fields, and Σ_u and Σ_d arise from the radiative corrections to the Higgs potential with dominant contribution to Σ_u given by

$$\Sigma_u \sim \frac{3Y_t^2}{16\pi^2} \times m_{\tilde{t}_i}^2 \left(\log \frac{m_{\tilde{t}_i}^2}{Q^2} - 1 \right). \quad (8)$$

These two equations indicate that, if the individual terms on the right hand side of Eq. (7) are comparable in magnitude so that the observed value of M_Z is obtained without resorting to large cancelations, relatively light stops and μ of $\mathcal{O}(100\text{GeV})$ are preferred. As far as the NMSSM and the nMSSM are concerned, due to the Higgs self interactions, the squared mass of the SM-like Higgs boson gets an additional contribution $\lambda^2 v^2 \sin^2 2\beta$ (compared with its MSSM expression), and further it can be enhanced by the doublet-singlet mixing [25, 32]. Consequently, predicting a 125GeV Higgs boson does not necessarily require heavy scalar top quarks[12]. This is very helpful in reducing the tuning. For example, it has been shown that the fine tuning parameter Δ , which is defined by $\Delta = \text{Max}\{|\partial \ln m_Z / \partial \ln p_i^{\text{GUT}}|\}$ with p_i^{GUT} denoting SUSY parameter at GUT scale [31]), may be as low as 4 in the two models, while in the MSSM it usually exceeds 100 [33].

About the nMSSM, one should note that the tadpole term in Eq.(6) only affects the Higgs masses and the minima of the scalar potential, so the interactions in the Higgs and neutralino sectors of the nMSSM are identical to those in the NMSSM with $\kappa = 0$. This enables us to modify the package **NMSSMTools** [34] and use it to study the phenomenology of the nMSSM [35]. Also note that the singlino mass vanishes at tree level and the lightest

neutralino as the dark matter candidate acquires its mass through the mixing of the singlino with Higgsinos and gauginos. In this case, the dark matter is light and singlino dominated, and it must annihilate through exchanging a resonant light CP-odd Higgs boson to get the correct relic density[35]. As a result, the SM-like Higgs boson will decay dominantly into light neutralinos or other light Higgs bosons so that the branching fractions of the visible decay channels like $h \rightarrow \gamma\gamma$, $b\bar{b}$, $ZZ^*(4l)$, $\tau^+\tau^-$ are suppressed[35]. This is strongly disfavored by current LHC data as shown in[33]. In this work, we only take the nMSSM as an example to show its peculiar behaviors in Higgs physics (in comparison with other new SUSY models).

Formula in calculation: In order to study the $h \rightarrow Z\gamma$ decay and its correlation with the $h \rightarrow \gamma\gamma$ decay in SUSY, we define following normalized rates at the LHC and the international linear collider (ILC)[21] as

$$R_{Z\gamma} \equiv \frac{\sigma(pp \rightarrow h \rightarrow Z\gamma)}{\sigma_{\text{SM}}(pp \rightarrow h \rightarrow Z\gamma)} = \frac{\sigma_{\text{tot}}}{\sigma_{\text{tot}}^{\text{SM}}} \frac{\text{Br}(h \rightarrow Z\gamma)}{\text{Br}_{\text{SM}}(h \rightarrow Z\gamma)} \simeq \left(\frac{C_{hgg}}{C_{hgg}^{\text{SM}}} \right)^2 \cdot \frac{\Gamma_{Z\gamma}(h)}{\Gamma_{Z\gamma}^{\text{SM}}(h)} \cdot \frac{\Gamma_{\text{tot}}^{\text{SM}}(h)}{\Gamma_{\text{tot}}(h)}, \quad (9)$$

$$R_{\gamma\gamma} \equiv \frac{\sigma(pp \rightarrow h \rightarrow \gamma\gamma)}{\sigma_{\text{SM}}(pp \rightarrow h \rightarrow \gamma\gamma)} = \frac{\sigma_{\text{tot}}}{\sigma_{\text{tot}}^{\text{SM}}} \frac{\text{Br}(h \rightarrow \gamma\gamma)}{\text{Br}_{\text{SM}}(h \rightarrow \gamma\gamma)} \simeq \left(\frac{C_{hgg}}{C_{hgg}^{\text{SM}}} \right)^2 \cdot \frac{\Gamma_{\gamma\gamma}(h)}{\Gamma_{\gamma\gamma}^{\text{SM}}(h)} \cdot \frac{\Gamma_{\text{tot}}^{\text{SM}}(h)}{\Gamma_{\text{tot}}(h)}, \quad (10)$$

$$\mathcal{K}_{Z\gamma} \equiv \frac{\sigma(e^+e^- \rightarrow Zh \rightarrow ZZ\gamma)}{\sigma_{\text{SM}}(e^+e^- \rightarrow Zh \rightarrow ZZ\gamma)} \simeq \left(\frac{C_{hZZ}}{C_{hZZ}^{\text{SM}}} \right)^2 \cdot \frac{\Gamma_{Z\gamma}(h)}{\Gamma_{Z\gamma}^{\text{SM}}(h)} \cdot \frac{\Gamma_{\text{tot}}^{\text{SM}}(h)}{\Gamma_{\text{tot}}(h)}, \quad (11)$$

$$\mathcal{K}_{b\bar{b}} \equiv \frac{\sigma(e^+e^- \rightarrow Zh \rightarrow Zb\bar{b})}{\sigma_{\text{SM}}(e^+e^- \rightarrow Zh \rightarrow Zb\bar{b})} \simeq \left(\frac{C_{hZZ}}{C_{hZZ}^{\text{SM}}} \right)^2 \cdot \frac{\Gamma_{b\bar{b}}(h)}{\Gamma_{b\bar{b}}^{\text{SM}}(h)} \cdot \frac{\Gamma_{\text{tot}}^{\text{SM}}(h)}{\Gamma_{\text{tot}}(h)}, \quad (12)$$

where the Higgs production at the LHC is dominated by the gluon fusion process, while at the ILC with $\sqrt{s} \sim 250\text{GeV}$, it is dominated by the Zh associated production. Here C_{hgg} and C_{hZZ} are the couplings of the Higgs boson to gluons and Z s respectively, and $\Gamma_{Z\gamma}(h)$, $\Gamma_{\gamma\gamma}(h)$ and $\Gamma_{b\bar{b}}(h)$ are the partial widths for the decays $h \rightarrow Z\gamma$, $h \rightarrow \gamma\gamma$ and $h \rightarrow b\bar{b}$ respectively. In getting these formulae, we neglect SUSY radiative corrections to the signals. Those corrections are expected to be few percent given that heavy sparticles are preferred by current LHC experiments.

In SUSY, the decays $h \rightarrow Z\gamma$ and $h \rightarrow \gamma\gamma$ get new contributions from the loops mediated by charged Higgs bosons, sfermions (including stops, sbottoms and staus) as well as

charginos. Consequently, the formula of $\Gamma_{Z\gamma}$ and $\Gamma_{\gamma\gamma}$ are modified by

$$\Gamma_{Z\gamma}(h) = \frac{G_F^2 m_W^2 \alpha m_h^3}{64 \pi^4} \left(1 - \frac{m_Z^2}{m_h^2}\right)^3 \left| \mathcal{A}_W^{Z\gamma} + \mathcal{A}_t^{Z\gamma} + \mathcal{A}_{\tilde{f}}^{Z\gamma} + \mathcal{A}_{H^\pm}^{Z\gamma} + \mathcal{A}_{\chi^\pm}^{Z\gamma} \right|^2, \quad (13)$$

$$\Gamma_{\gamma\gamma}(h) = \frac{G_F \alpha^2 m_h^3}{128 \sqrt{2} \pi^3} \left| \mathcal{A}_W^{\gamma\gamma} + \mathcal{A}_t^{\gamma\gamma} + \mathcal{A}_{\tilde{f}}^{\gamma\gamma} + \mathcal{A}_{H^\pm}^{\gamma\gamma} + \mathcal{A}_{\chi^\pm}^{\gamma\gamma} \right|^2, \quad (14)$$

where \mathcal{A}_i ($i = W, t, \tilde{f}, H^\pm, \chi^\pm$) denote the contribution from particle i mediated loops, and their explicit expressions are listed in the Appendix. Note that our expressions differ from those presented in [36] in two aspects. One is that we have an overall minus sign for the new contributions \mathcal{A}_{H^\pm} , $\mathcal{A}_{\tilde{f}}$ and \mathcal{A}_{χ^\pm} , and an additional factor 2 for the sfermion contributions. This sign difference was also observed recently in [37]. The other difference is that we have included in a neat way the contributions from the loops with two particles (such as \tilde{f}_1 and \tilde{f}_2 or χ_1^\pm and χ_2^\pm) running in them. Such contributions were considered to be negligibly small [36], but our results indicate that sometimes they may play a role. Also note that in the SUSY package FeynHiggs [38], the decay $h \rightarrow Z\gamma$ is not calculated. In the package NMSSMTools [34], this decay is calculated only by considering the contributions from the SM particles and the charged Higgs boson. We improve these packages by inserting our codes for $h \rightarrow Z\gamma$.

III. NUMERICAL CALCULATION AND DISCUSSIONS

In our calculation, we first perform a random scan over the parameter space of each model by considering various experimental constraints. Then for the surviving samples we investigate the $h \rightarrow Z\gamma$ and $h \rightarrow \gamma\gamma$ decays. Since for each unconstrained SUSY model, there are too many free parameters involved in the calculation we make some assumptions to simplify our analysis. Our treatment of the MSSM and the NMSSM is as follows

- Firstly, we note that the first two generation squarks change little the properties of the Higgs boson, and the LHC search for SUSY particles implies that they should be very heavy. So in our scan, we fix all soft masses and the trilinear parameters in this sector to be 2 TeV. We checked that our conclusions are not affected by such specific choice.
- Secondly, since the third generation squarks affect the Higgs sector significantly, we set

free all soft parameters in this sector except that we assume $m_{U_3} = m_{D_3}$ and $A_t = A_b$ to reduce the number of free parameters.

- Thirdly, considering that the muon anomalous magnetic moment is sensitive to the spectrum of scalar muons and the decay $h \rightarrow Z\gamma$ may get significant contribution from scalar tau (stau) sector, we assume $A_\tau = A_\mu = A_e = 0$, $M_{L_3} = M_{L_2} = M_{L_1}$ and $M_{E_3} = M_{E_2} = M_{E_1}$, and treat M_{L_3} and M_{E_3} as free parameters. We checked that for our considered cases, the decay $h \rightarrow Z\gamma$ is insensitive to A_τ .
- Finally, since our results are insensitive to gluino mass, we fix it at 2 TeV. We also assume the grand unification relation $3M_1/5\alpha_1 = M_2/\alpha_2$ for electroweak gaugino masses.

To sum up, for the MSSM we scan the parameters in the following regions

$$\begin{aligned}
1 \leq \tan \beta \leq 60, \quad 100 \text{ GeV} \leq \mu \leq 1 \text{ TeV}, \quad 100 \text{ GeV} \leq M_A \leq 1 \text{ TeV}, \\
100 \text{ GeV} \leq (M_{Q_3}, M_{U_3}) \leq 2 \text{ TeV}, \quad 100 \text{ GeV} \leq (M_{L_3}, M_{E_3}) \leq 1 \text{ TeV}, \\
-3 \text{ TeV} \leq A_t \leq 3 \text{ TeV}, \quad 50 \text{ GeV} \leq M_1 \leq 500 \text{ GeV}.
\end{aligned} \tag{15}$$

Note that in actual calculation λ and μ_{eff} in the NMSSM are usually treated as independent input parameters, and for any given value of μ_{eff} the phenomenology of the NMSSM is identical to that of the MSSM with $\mu = \mu_{eff}$ in the limit $\lambda, \kappa \rightarrow 0$ [25]. This enables us to use the package NMSSMTools [34], which calculates various observables and also considers various experimental constraints in the framework of the NMSSM, to study the phenomenology of the MSSM (note that the validity of this method has been justified by the authors of the NMSSMTools [34]). In our calculation we use the package NMSSMTools-3.2.4 to perform the scan for the MSSM by setting $\lambda = \kappa = 10^{-4}$ and $A_\kappa = -10\text{GeV}$. Here the value of A_κ is actually irrelevant to our calculation for the MSSM as long as it is negative and satisfies $|A_\kappa| < 4\kappa\mu/\lambda$ (in order to guarantee the squared masses of the singlet scalars to be positive) [25].

For the NMSSM, we use the package NMSSMTools-3.2.4 to scan the region in Eq.(15) and also following ranges for additional parameters

$$0.5 \leq \lambda \leq 0.7, \quad 0 \leq \kappa \leq 0.7, \quad |A_\kappa| \leq 1 \text{ TeV}. \tag{16}$$

Note that in our scan, we only consider a relatively large λ . The reason is in the NMSSM, the properties of the SM-like Higgs boson are expected to deviate significantly from the MSSM prediction only for a sizable λ [25], and in particular, as far as $\lambda \gtrsim 0.5$ is concerned, the Higgs mass at tree level is maximized at $\tan\beta \simeq 1$, instead of at large $\tan\beta$ in the MSSM.

As for the nMSSM, our assumptions are same as those for the MSSM except that, in order to explain the muon anomalous magnetic moment at 2σ level, we assume all soft SUSY breaking parameters in slepton sector to be 100 GeV [35]. Such a slepton mass is allowed by the LEP II bounds, which are 99.9 GeV for the first two generations and 93.2 GeV for the third generation [39]. Although the LHC also gave a bound on slepton mass by searching for the decay $\tilde{l} \rightarrow l\tilde{\chi}_1^0 \rightarrow l + \cancel{E}$ [40, 41], it is not applicable to the nMSSM. The reason is that in the nMSSM, the LSP is singlino-like and the NLSP is usually a bino-like neutralino $\tilde{\chi}_2^0$. As a result, the dominant decay chain of a slepton is $\tilde{l} \rightarrow l\tilde{\chi}_2^0 \rightarrow l\tilde{\chi}_1^0 A \rightarrow l\tilde{\chi}_1^0 b\bar{b} \rightarrow l + \cancel{E} + jets$ [35]. Other parameters in this model are scanned in the following ranges

$$0.1 \leq \lambda \leq 0.7, \quad |A_\lambda| \leq 1 \text{ TeV}, \quad 0 \leq \tilde{m}_S \leq 200 \text{ GeV}, \quad (17)$$

where \tilde{m}_S is the soft breaking mass for the singlet Higgs field. In our calculation, we adapt the code of the NMSSMTools to the nMSSM case as done in[35].

For the CMSSM, we use the package NMSPEC[42] to scan following parameter space

$$100 \text{ GeV} \leq (M_0, M_{1/2}) \leq 2 \text{ TeV}, \quad 1 \leq \tan\beta \leq 60, \quad -3 \text{ TeV} \leq A_0 \leq 3 \text{ TeV}, \quad (18)$$

and we take the sign of μ to be positive. Similar to the MSSM scan, we set $\lambda = \kappa = 10^{-4}$ and $A_\kappa = -10\text{GeV}$ at the GUT scale (note that the validity of the NMSPEC to study the phenomenology of the CMSSM was emphasized by the authors of the package [42]).

Since in the CMSSM different soft breaking parameters at electroweak scale are correlated, it is expected that its phenomenology CMSSM is only a subset of the MSSM.

In our scan we have considered various constraints on the models, which are from vacuum stability, the LEP and LHC searches for SUSY particles and Higgs bosons, the electroweak observables ϵ_i and R_b , B physics observables such as the branching ratio of $B \rightarrow X_s \gamma$ and the mass difference ΔM_s , the dark matter relic density and its direct detection experiments. When imposing the constraint from a certain observable which has experimental central value, we require SUSY to explain the observable at 2σ level. These constraints are described

in detail in [43] and have been implemented in the package NMSSMTools-3.2.4 [34]. In particular, the dark matter relic density is calculated by the package MicrOMEGAs [44], which now acts as an important component of the NMSSMTools.

Compared with the constraints in [43], we have following improvement in this work

- We require $123\text{GeV} \leq m_h \leq 127\text{GeV}$. This mass range is favored by the LHC search for Higgs boson after considering theoretical uncertainties[1, 2].
- We utilize the latest result of the XENON100 experiment to limit the models (at 90% confidence level)[45]. We calculate the scattering cross section of the dark matter with nucleon with the formula presented in [43], and we set $f_{T_s} = 0.020$ with f_{T_s} denoting the strange quark content in nucleon.
- We consider the constraints from the recent LHCb measurement of $B_s \rightarrow \mu^+\mu^-$, which is $\text{Br}(B_s^0 \rightarrow \mu^+\mu^-) = (3.2_{-1.2}^{+1.5}) \times 10^{-9}$ [46]. The agreement of the measurement with its SM prediction strongly limits the combination $\tan^6 \beta/M_A^4$ in the MSSM[47].
- We also consider the constraint from the CMS search for non-SM Higgs boson from the channel $H/A \rightarrow \tau^+\tau^-$ [48]. This search, like $B_s^0 \rightarrow \mu^+\mu^-$, is very power in limiting the $\tan \beta - M_A$ plane in the MSSM.

Finally, we emphasize that in our scan we require the MSSM, NMSSM and nMSSM to explain muon g-2 at 2σ level, i.e., $a_\mu^{exp} - a_\mu^{SM} = (25.5 \pm 8.0) \times 10^{-10}$ [49]. As for the CMSSM, it has long been noticed that there exists a tension to predict a 125 GeV SM-like Higgs boson and meanwhile to explain the muon g-2 [50–52]. In our calculation we consider the latest LHC bounds on $M_0 - M_{1/2}$ plane of CMSSM and find that under such latest bounds the CMSSM cannot explain the muon g-2 at 2σ level. So we do not require the CMSSM to explain the muon g-2 at 2σ level in our analysis.

In Fig.1 we project the surviving samples on the plane of the $Z\gamma$ signal rate at the LHC versus the SM-like Higgs boson mass in the four SUSY models. We also show the CMS bound on the rate in the figure [20]. From the left panel we see that compared with its SM prediction, the $Z\gamma$ rate in the MSSM and the NMSSM can be either enhanced or suppressed with the maximal deviation reaching 20% and 60% respectively. In contrast, as shown in the right panel, the $Z\gamma$ rate is always slightly suppressed (less than 5%) in the CMSSM and severely suppressed (more than 90%) in the nMSSM. We checked that for the CMSSM and

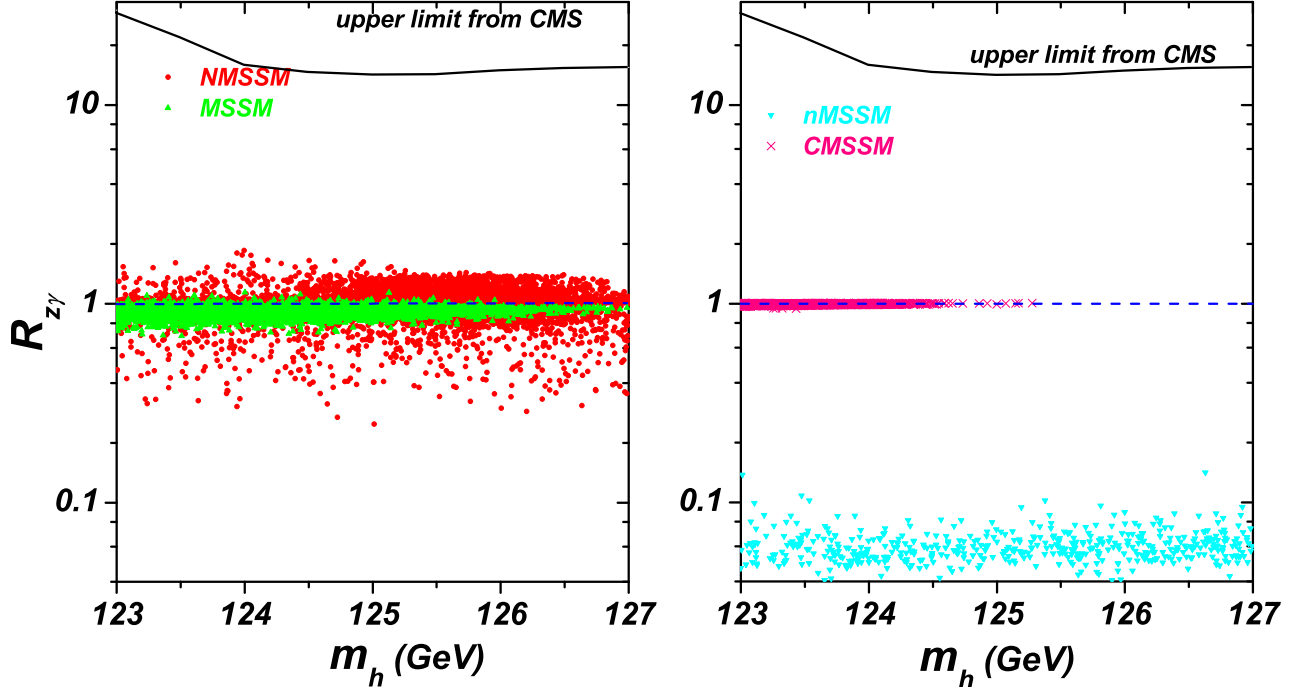


FIG. 1: The scatter plots of the surviving samples in the four models, projected on the $R_{Z\gamma} - m_h$ plane. Here $R_{Z\gamma} = \sigma(pp \rightarrow h \rightarrow Z\gamma)/\sigma_{\text{SM}}(pp \rightarrow h \rightarrow Z\gamma)$ denotes the normalized $Z\gamma$ signal rate in the SM-like Higgs boson production at the LHC, and the black line represents its upper limit set by the CMS collaboration [20].

the MSSM, the suppression is mainly due to the increase of $h \rightarrow b\bar{b}$ partial width [12, 53]. For the nMSSM, however, it is due to the open up of new decays $h \rightarrow \chi^0\chi^0, a_1a_1$ (χ^0 and a_1 denote the dark matter and lightest CP-odd higgs boson respectively), which significantly enlarges the total width of the Higgs boson and leads to severe suppression for all visible decay channels.

For the samples shown in Fig.1, we also compare their predictions on the $\gamma\gamma$ and ZZ^* signal rates of the Higgs boson with the corresponding experimental data. We find that for most of the samples in the MSSM and the NMSSM and for all the samples in the CMSSM, their theoretical predictions on the $\gamma\gamma$ and ZZ^* rates agree with the corresponding data at 3σ level, while for the samples in the nMSSM, their predictions always lie outside the 3σ regions (see Fig.1 and Fig.2 in [33]). Moreover, we checked that the branching ratio of $h \rightarrow b\bar{b}$ in the MSSM, NMSSM and CMSSM varies in the ranges [57%, 69%], [32%, 67%] and [60%, 63%], respectively (in the SM its value is about 57% for $m_h \simeq 125.5\text{GeV}$), and the signal strength for the process $pp \rightarrow Vh \rightarrow Vb\bar{b}$ normalized by its SM value varies from 0.97

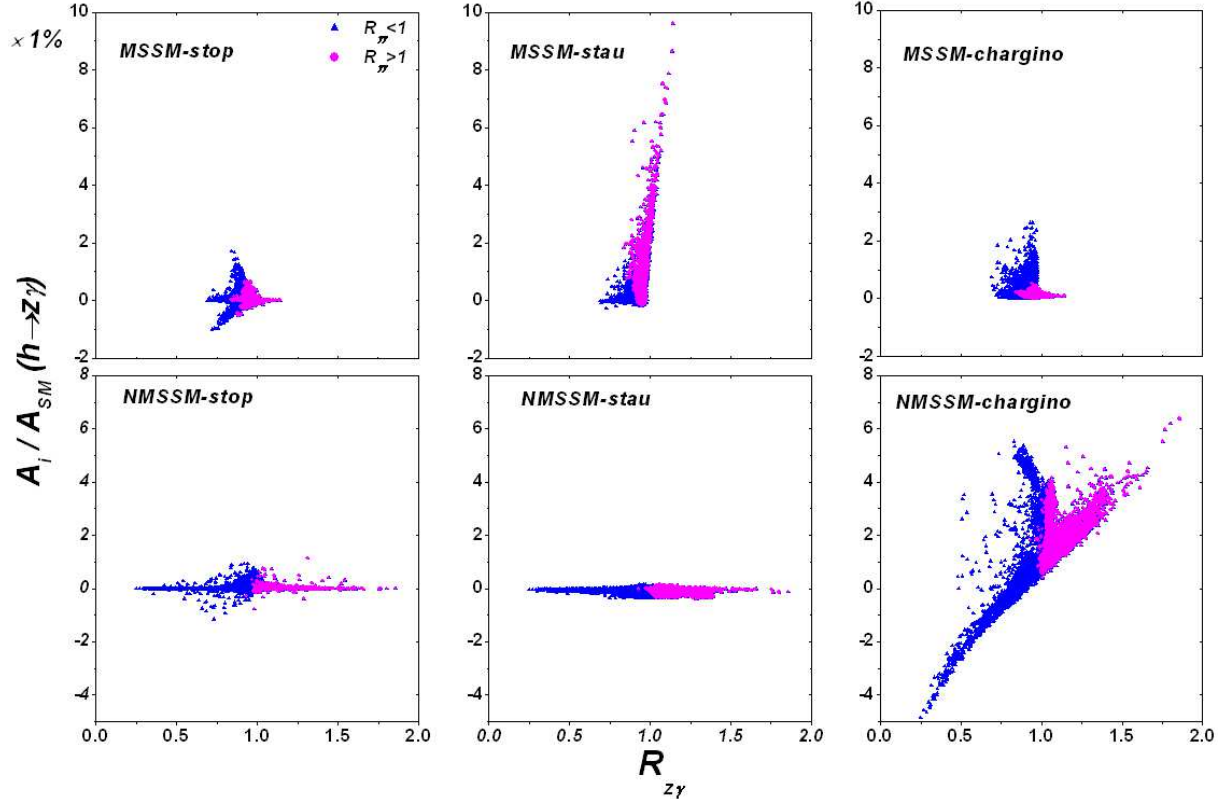


FIG. 2: Same as Fig.1, but showing the normalized sparticle contributions to the amplitude of $h \rightarrow Z\gamma$ in the MSSM and NMSSM. The magenta bullets and blue triangles represent the samples with $R_{Z\gamma} > 1$ and $R_{Z\gamma} < 1$ respectively.

to 1.12, 0.55 to 1.05 and 1.00 to 1.02, respectively. Considering that so far the only way to detect the $h \rightarrow b\bar{b}$ decay at the LHC is through the Vh associated production, whose signal strength $\mu_{Vb\bar{b}}$ is -0.4 ± 1.0 from ATLAS result [54] and 1.0 ± 0.49 from CMS result [55], one can conclude that such alterations of $b\bar{b}$ signal rates are allowed by the current experimental data at 2σ level.

Next we focus on the MSSM and the NMSSM. In Fig.2 we exhibit the contributions of different sparticles to the amplitude of the $h \rightarrow Z\gamma$ decay. Since the sbottoms and charged Higgs bosons have little effect on the amplitude, we do not show their contributions. This figure shows following features:

- (1) In the MSSM, the potentially largest contribution comes from the stau loops, which can alter the SM amplitude by about 10%. In contrast, the stop contribution is small, which usually changes the amplitude by less than 3%. This feature can be well understood by the formulae listed in Appendix. Explicitly speaking, in order to get a

significant sfermion contribution, one necessary condition is $Y_{hLR} \sin 2\theta_{\tilde{f}}/m_{\tilde{f}_1}^2$ should be as large as possible, where Y_{hLR} denotes the chiral flipping coupling of Higgs to sfermions, $\theta_{\tilde{f}}$ is the chiral mixing angle and $m_{\tilde{f}_1}$ represents the lighter sfermion mass. As far as the stop sector is concerned, a relatively light \tilde{t}_1 is always accompanied by a heavy \tilde{t}_2 in order to predict $m_h \simeq 125\text{GeV}$. Although A_t in this case may be very large, the chiral mixing angle $\theta_{\tilde{t}}$ is usually small and consequently, the stop contribution can never get significantly enhanced. In the stau sector, however, both the parameters M_{L3} and M_{E3} are unlimited, and one can choose light staus and an appropriate $\theta_{\tilde{\tau}}$ to maximize the contribution. In this process, the value of $\mu \tan \beta$ and the splitting between M_{L3} and M_{E3} play an important role. It is worth noting that a light stau with mass close to dark matter may co-annihilate with the dark matter, which is helpful to avoid the overabundance of the dark matter in today's universe[56, 57].

- (2) In the MSSM, the chargino contribution is small and can only reach 3% and 0.5% for $R_{\gamma\gamma} < 1$ case and $R_{\gamma\gamma} > 1$ case respectively. The reason is that in the MSSM, the $h\chi_1^+\chi_1^-$ coupling is induced by the $H_i^0\tilde{H}\tilde{W}$ interaction ($i = u, d$ and \tilde{H} and \tilde{W} denote Higgsino and Wino respectively), and this coupling strength is maximized when both the Higgsino and Wino components of χ_1^\pm are sizable. We checked that, for most of the $R_{\gamma\gamma} > 1$ samples, $M_2 \leq 700\text{GeV}$ and $\mu > 800\text{GeV}$ (a large μ is needed for the stau contribution to enhance the diphoton rate [12]) so that χ_1^\pm is basically Wino-like. Consequently, its coupling to the Higgs boson is weak.
- (3) In the NMSSM, the largest SUSY contribution to the $Z\gamma$ decay comes from the chargino loops with the correction reaching 6% in optimal case, while the magnitude of the stau contribution is always smaller than 1%. This is because in the NMSSM with a large λ , μ is preferred to vary from 100 GeV to 250 GeV and $\tan \beta$ is usually smaller than 10 [31]. As a result, the $h\tilde{\chi}_1^\pm\chi_1^\pm$ coupling is relatively large, while the $h\tilde{\tau}_L^*\tilde{\tau}_R$ coupling can not be pushed up by the moderate $\mu \tan \beta$. Due to the singlet component of h in the NMSSM, the $h\tilde{b}\tilde{b}$ coupling can be greatly suppressed (reaching 40% by our results) so that the total width of h is reduced by about 50% in extreme case[33]. Consequently, even when the SUSY contributions to the decay width are small, $R_{Z\gamma}$ can still be quite large. As we mentioned before, such a suppressed $h\tilde{b}\tilde{b}$ coupling can reduce the normalized strength of the process $pp \rightarrow Vh \rightarrow Vb\bar{b}$ down to

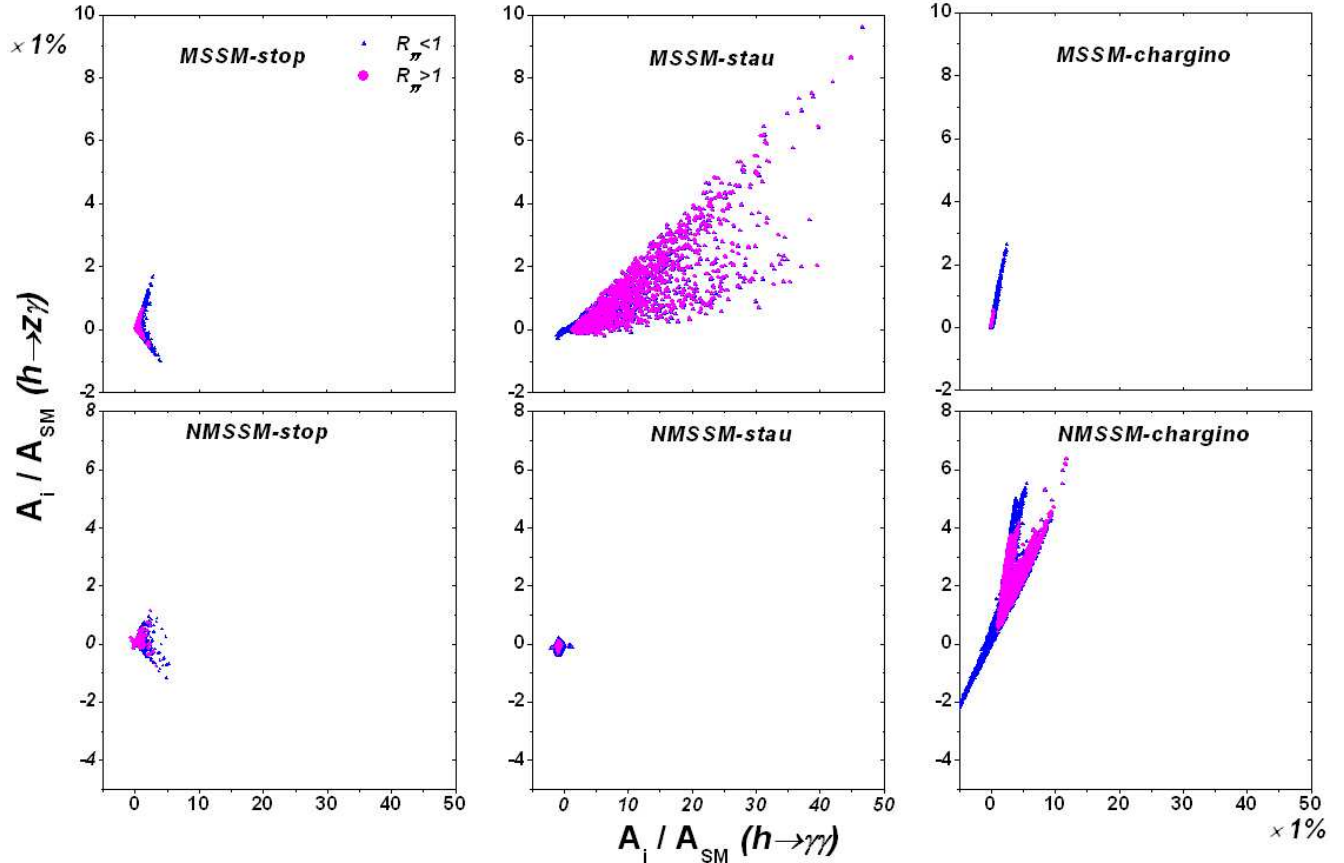


FIG. 3: Same as Fig.2, but showing the correlation of SUSY particle contribution to $h \rightarrow Z\gamma$ channel with that to $h \rightarrow \gamma\gamma$ channel.

0.55, which, however, is still compatible with the current LHC data due to the large uncertainty of the measured signal strength ($\mu_{Vb\bar{b}} = -0.4 \pm 1.0$ from ATLAS result [54] and $\mu_{Vb\bar{b}} = 1.0 \pm 0.49$ from CMS result [55]).

In Fig.3, we show the correlation of the amplitudes for $h \rightarrow Z\gamma$ and $h \rightarrow \gamma\gamma$. This figure indicates that in both the MSSM and the NMSSM, the top squark contribution to the amplitude of $h \rightarrow Z\gamma$ correlates roughly in a linear way with that of $h \rightarrow \gamma\gamma$, and so is the chargino contribution. Fig.3 also indicates that the correlation is spoiled for the stau contribution in the MSSM. We checked that this is because θ_τ in the MSSM can vary over a broad range and the dependence of the two amplitudes on θ_τ are quite different. For example, in the case $M_{L3} \simeq M_{E3}$, $\theta_\tau \simeq \pi/4$ and both $Z\tilde{\tau}_i^*\tilde{\tau}_i$ and $h\tilde{\tau}_1^*\tilde{\tau}_2$ couplings approach zero by accidental cancellation. As a result, the stau contribution to the decay $h \rightarrow Z\gamma$ is suppressed. In contrast, the contribution to the decay $h \rightarrow \gamma\gamma$ is maximized since it is proportional to $\sin 2\theta_\tau$. On the other hand, if $|M_{L3}^2 - M_{E3}^2| \gg m_\tau \mu \tan \beta$ so that $\theta_\tau \rightarrow 0$,

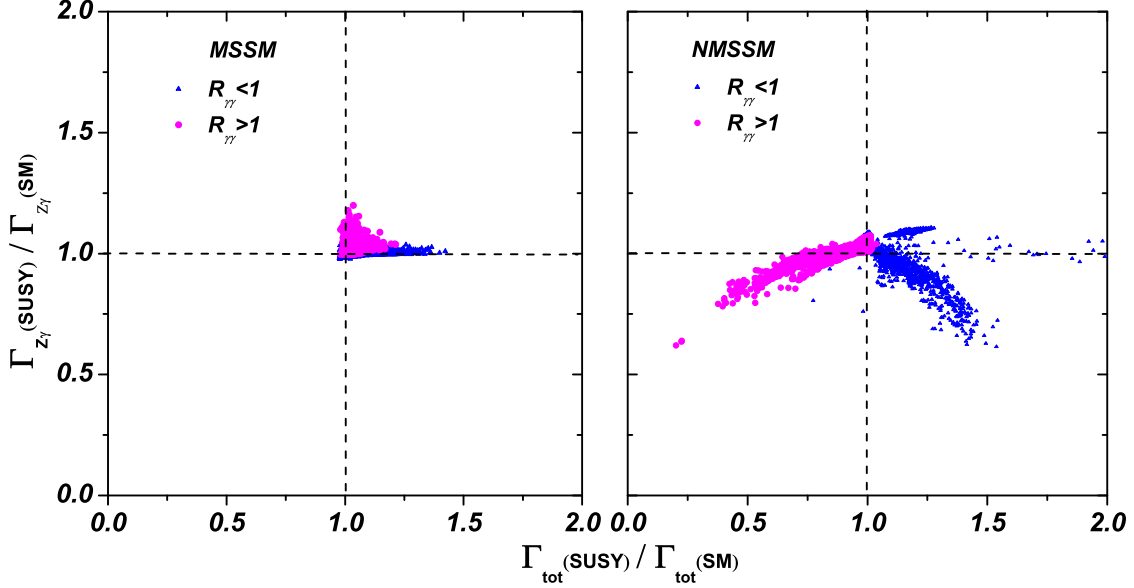


FIG. 4: Same as Fig.2, but projected on the plane of $\Gamma_{Z\gamma}^{\text{SUSY}}/\Gamma_{Z\gamma}^{\text{SM}}$ versus $\Gamma_{\text{total}}^{\text{SUSY}}/\Gamma_{\text{total}}^{\text{SM}}$.

the contributions are suppressed for both the decays because the dominant contribution to $Z\tilde{\tau}_1^*\tilde{\tau}_2$ coupling and that to $h\tilde{\tau}_i^*\tilde{\tau}_i$ coupling are both proportional to $\sin 2\theta_\tau$.

Considering $R_{Z\gamma}$ is mainly determined by the partial width of $h \rightarrow Z\gamma$ and the total width of the SM-like Higgs boson, we present in Fig.4 the ratio of $\Gamma_{Z\gamma}^{\text{SUSY}}/\Gamma_{Z\gamma}^{\text{SM}}$ versus the ratio of $\Gamma_{\text{total}}^{\text{SUSY}}/\Gamma_{\text{total}}^{\text{SM}}$ for the two models. The left panel indicates that for almost all MSSM samples the $Z\gamma$ partial width and the total width of the SM-like Higgs boson is larger than the corresponding SM predictions. These features originate from the constructive contributions of the SUSY particles to $h \rightarrow Z\gamma$ and the enhanced width of $h \rightarrow b\bar{b}$ respectively. Interestingly, the largest increase of $\Gamma_{Z\gamma}$ occurs when $\Gamma_{\text{total}}^{\text{SUSY}} \simeq \Gamma_{\text{total}}^{\text{SM}}$. The right panel indicates that, in order to enhance the $Z\gamma$ signal in the NMSSM with a large λ (note that in this model, $R_{Z\gamma}$ correlates roughly in a linear way with $R_{\gamma\gamma}$, see Fig.5), the SM-like Higgs boson tends to have sizable singlet component to suppress the total width. In this case, $\Gamma_{Z\gamma}$ is suppressed too, but we have $\Gamma_{Z\gamma}^{\text{SUSY}}/\Gamma_{Z\gamma}^{\text{SM}} > \Gamma_{\text{total}}^{\text{SUSY}}/\Gamma_{\text{total}}^{\text{SM}}$. Moreover, as mentioned before, $\Gamma_{Z\gamma}$ can be slightly enhanced by the chargino contribution.

Now we investigate the correlation of the $Z\gamma$ rate with the $\gamma\gamma$ rate in different SUSY models, which is shown in Fig.5. From this figure we have following conclusions:

- (a) In the MSSM, although the partial width of $h \rightarrow Z\gamma$ can be enhanced by 20% (see Fig.4), due to the increase of the Higgs total width and also the suppression of the

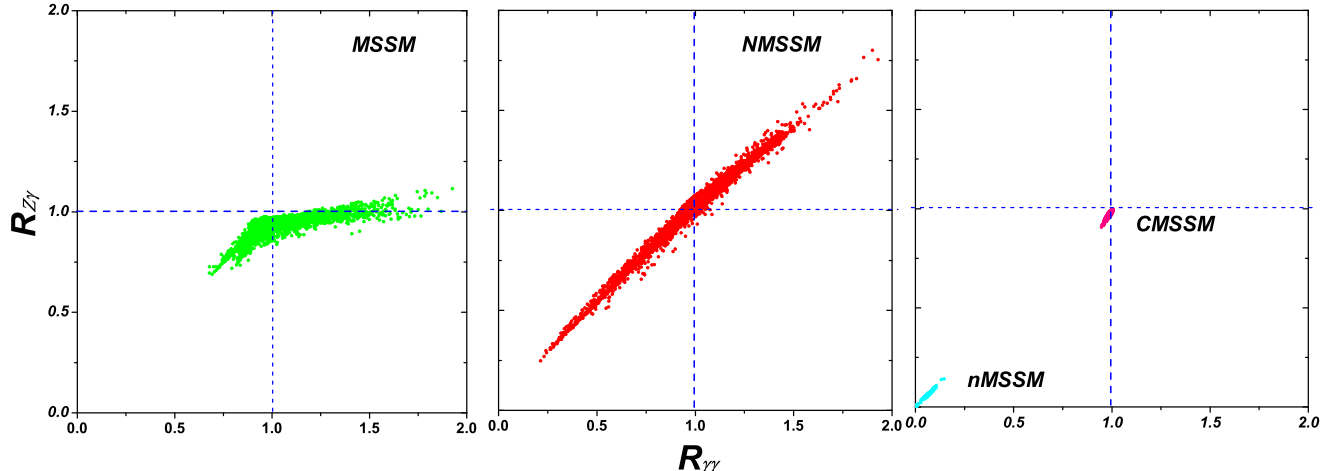


FIG. 5: Same as Fig.1, but showing the correlation between $R_{Z\gamma} = \sigma(pp \rightarrow h \rightarrow Z\gamma)/\sigma_{\text{SM}}(pp \rightarrow h \rightarrow Z\gamma)$ and $R_{\gamma\gamma} = \sigma(pp \rightarrow h \rightarrow \gamma\gamma)/\sigma_{\text{SM}}(pp \rightarrow h \rightarrow \gamma\gamma)$ in the four models.

hgg coupling [12], the maximal value of $R_{Z\gamma}$ is only 1.1 (in comparison, $R_{\gamma\gamma}$ may be as large as 2.), and only when $R_{\gamma\gamma} \gtrsim 1.25$ can $R_{Z\gamma} > 1$ be possible. Among the sparticle contributions to $R_{Z\gamma}$ and $R_{\gamma\gamma}$, the stau loops play the dominant role. The difference between the two signals comes from their dependence on θ_τ , i.e. $\theta_\tau \simeq \pi/4$ $R_{\gamma\gamma}$ is maximized while $R_{Z\gamma}$ is suppressed. Our numerical results also indicate that, for the surviving samples of the MSSM, the branching ratio of the invisible decay $h \rightarrow \chi^0\chi^0$ is usually smaller than 6% and 3% for $R_{\gamma\gamma} < 1$ and $R_{\gamma\gamma} > 1$ case, respectively, and the branching ratio of $h \rightarrow b\bar{b}$ varies from 57% to 69%.

- (b) In the NMSSM with a large λ , the sparticle corrections to the amplitudes of $h \rightarrow Z\gamma$ and $h \rightarrow \gamma\gamma$ are usually below 10%, and the main mechanism to alter $R_{Z\gamma}$ and $R_{\gamma\gamma}$ is through the suppression of the $hb\bar{b}$ and hW^+W^- couplings by the singlet component of h . As a result, $R_{Z\gamma}$ and $R_{\gamma\gamma}$ are highly correlated and both of them vary from 0.2 to 2. We checked that the branching ratios of the exotic decays $h \rightarrow \chi^0\chi^0, a_1a_1$ may reach 22% and 45%, respectively (these extreme cases correspond to some of the squared points in Fig.5 of [33]), and the branching ratio of the decay $h \rightarrow b\bar{b}$ varies in a large range, from 32% to 67%.
- (c) In the CMSSM and nMSSM, $R_{Z\gamma}$ and $R_{\gamma\gamma}$ are slightly and strongly suppressed respectively. As discussed before, in the CMSSM the suppression is due to the increase of $h \rightarrow b\bar{b}$ partial width, while in nMSSM it is due to the open up of the exotic decay

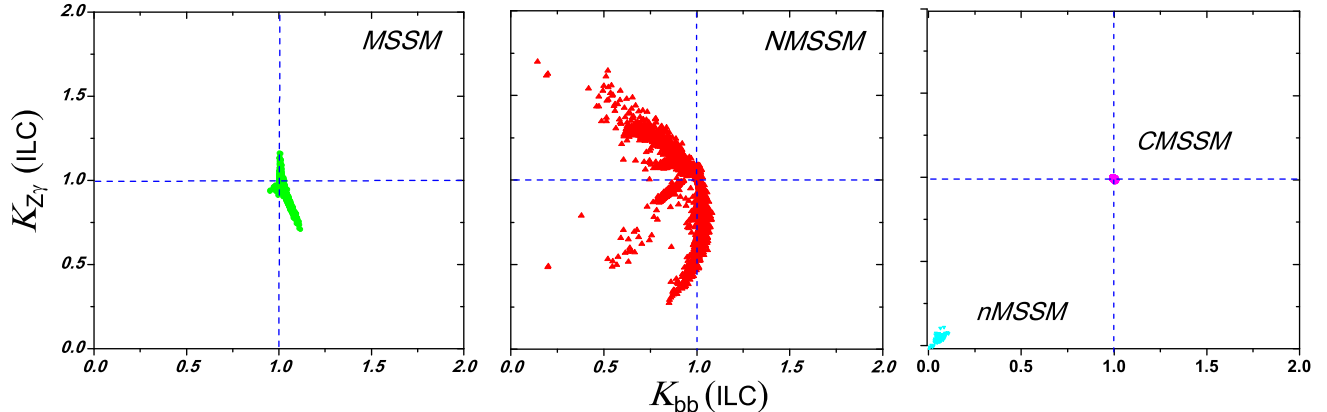


FIG. 6: Same as Fig.1, but showing the correlation between $\mathcal{K}_{Z\gamma} = \sigma(e^+e^- \rightarrow Zh \rightarrow ZZ\gamma)/\sigma_{\text{SM}}(e^+e^- \rightarrow Zh \rightarrow ZZ\gamma)$ and $\mathcal{K}_{b\bar{b}} = \sigma(e^+e^- \rightarrow Zh \rightarrow Zb\bar{b})/\sigma_{\text{SM}}(e^+e^- \rightarrow Zh \rightarrow Zb\bar{b})$ in the four models.

channels $h \rightarrow \chi^0\chi^0, a_1a_1$.

Note that the open up of the exotic decays $h \rightarrow \chi^0\chi^0, a_1a_1$ will generally lead to the suppression of visible signal rates such as $R_{\gamma\gamma}$ and R_{ZZ^*} , and as analyzed in [58], the latest Higgs data require that the total branching ratio of the exotic decays should be less than 28% at 95% C.L.. This conclusion again indicates that the nMSSM and also some samples of the NMSSM are disfavored by the current Higgs data (about this conclusion, one may also see the squared points in Fig.5 of [33]). For the decay $h \rightarrow a_1a_1$ in the NMSSM, we checked that m_{a_1} varies from about 20GeV to 60GeV, and a_1 mainly decays to $b\bar{b}$ (with a branching ratio at about 90%) and $\tau\bar{\tau}$ (with the branching ratio at about 9%). So in this case, the decay product of the Higgs boson is four b -jets, or four τ leptons or two b -jets plus two τ leptons, which is an interesting but challenging signal in Higgs search at the LHC[59]. Since m_{a_1} is usually heavier than Υ , the constraint from the decay $\Upsilon \rightarrow a_1\gamma$ [60] is irrelevant here. Also note that generally speaking, the constrained model such as CMSSM tends to predict strong correlations among observables due to the unified nature of its parameters. This is clearly shown in Fig.5 for the CMSSM in comparison with the other three models.

Since the e^+e^- collider at $\sqrt{s} \sim 250\text{GeV}$ provides a clean environment to detect the decays $h \rightarrow Z\gamma$ and $h \rightarrow b\bar{b}$, we also investigate their rates at the ILC defined in Eq.(11) and Eq.(12). The corresponding results are shown in Fig.6. This figure exhibits following features

- (a) In the MSSM, a suppressed $Z\gamma$ signal (compared with its SM prediction) tends to correspond to an enhanced $b\bar{b}$ signal, and an enhanced $Z\gamma$ signal requires the $b\bar{b}$ signal rates to be roughly at its SM prediction. In any case, the enhancement factor for the two signals are less than 1.2. Note that there exist a few cases where the $b\bar{b}$ signal rate is slightly suppressed.
- (b) In the NMSSM with a large λ , the normalized $b\bar{b}$ signal rate is less than 1.1, and in some cases it may be significantly suppressed. In contrast, the $Z\gamma$ signal rate can be either greatly enhanced or severely suppressed. In the enhancement case, the $b\bar{b}$ signal rate is usually less than its SM prediction, and the greater enhancement corresponds to the stronger suppression.
- (c) In the CMSSM, both the signal rates are roughly equal to their SM predictions. In the nMSSM, however, both the rates are strongly suppressed.

Moreover, we checked that the $\gamma\gamma$ signal rate at the ILC has similar dependence on the $b\bar{b}$ rate for the four models.

IV. CONCLUSION

In this work, we investigate the rare decay of the SM-like Higgs boson, $h \rightarrow Z\gamma$, and study its correlation with $h \rightarrow \gamma\gamma$ in the MSSM, the NMSSM, the nMSSM and the CMSSM. We perform a scan over the parameter space of each model by considering various experimental constraints and present our results on various planes. We have following observations:

- (i) In the SUSY models, the sparticle correction to the rare decay $h \rightarrow Z\gamma$ is usually several times smaller than that to $h \rightarrow \gamma\gamma$.
- (ii) In the MSSM, the net SUSY contribution to the amplitude of $h \rightarrow Z\gamma$ is constructive with the corresponding SM amplitude and can enhance the SM prediction by at most 10%. As a result, the $Z\gamma$ signal rates at the LHC and the ILC can be enhanced by 20% at most. As a comparison, the $\gamma\gamma$ rate can be enhanced by a factor of 2 due to the large stau contributions.
- (iii) In the CMSSM, due to the slightly enhanced total width of the SM-like Higgs boson, the

$Z\gamma$ signal rates at the LHC and the ILC are both slightly below their SM predictions, and so is the $\gamma\gamma$ signal.

- (iv) In the NMSSM with a large λ , the SUSY corrections to the amplitudes for the decays $h \rightarrow Z\gamma$ and $h \rightarrow \gamma\gamma$ are at most 10%, and to get significant deviation of the two rates from their SM values, the total width of the SM-like Higgs boson must be moderately suppressed by the singlet component of h . In this model, the two rates are highly correlated and vary from 0.2 to 2.
- (v) In the nMSSM, the signal rates of $h \rightarrow Z\gamma$ and $h \rightarrow \gamma\gamma$ are both greatly suppressed due to the open up of the exotic decay $h \rightarrow \chi^0\chi^0, a_1a_1$.

Finally, we note that some strategies have been proposed in the literature to discriminate the considered models, e.g., via the correlations between the Higgs couplings [33], via the enhanced Higgs pair productions at the LHC [61] and the ILC [62], or via the direct dark matter detection [43]. Compared with these existing strategies, the loop-induced $Z\gamma$ and $\gamma\gamma$ decay modes of the Higgs boson seem to be more sensitive to the nature of the models (some non-SUSY models predict rather different correlation behavior [7]). So the correlation between $Z\gamma$ and $\gamma\gamma$ rates analyzed in this work may play a complementary role to discriminate new physics models in the future.

Note added: After we finished this work, both the ATLAS and CMS collaborations updated their Higgs search results [63, 64]. Among these new results, the CMS data on the diphoton signal rate is changed significantly [64]. Since in our analysis we did not use the diphoton data as a constraint (instead we just displayed the predictions for the diphoton signal rate in different SUSY models), our results and conclusions are not affected by the new data.

Acknowledgement

We thank Kun Yao and Jingya Zhu for helpful discussions. This work was supported in part by the National Natural Science Foundation of China (NNSFC) under grant No. 10775039, 11075045, 11275245, 10821504 and 11135003, by the Project of Knowledge Innovation Program (PKIP) of Chinese Academy of Sciences under grant No. KJCX2.YW.W10.

Appendix

In SUSY, the decays $h \rightarrow Z\gamma$ and $h \rightarrow \gamma\gamma$ get new contributions from the loops mediated by charged Higgs bosons, sfermions (including stops, sbottoms and staus) and charginos, and as a result, the formula of $\Gamma_{Z\gamma}$ and $\Gamma_{\gamma\gamma}$ are modified by

$$\Gamma(h \rightarrow Z\gamma) = \frac{G_F^2 m_W^2 \alpha m_h^3}{64 \pi^4} \left(1 - \frac{m_Z^2}{m_h^2}\right)^3 \left| \mathcal{A}_W^{Z\gamma} + \mathcal{A}_t^{Z\gamma} + \mathcal{A}_{H^\pm}^{Z\gamma} + \mathcal{A}_{\tilde{f}_i}^{Z\gamma} + \mathcal{A}_{\chi_i^\pm}^{Z\gamma} \right|^2 \quad (19)$$

$$\Gamma(h \rightarrow \gamma\gamma) = \frac{G_F \alpha^2 m_h^3}{128 \sqrt{2} \pi^3} \left| \mathcal{A}_W^{\gamma\gamma} + \mathcal{A}_t^{\gamma\gamma} + \mathcal{A}_{H^\pm}^{\gamma\gamma} + \mathcal{A}_{\tilde{f}_i}^{\gamma\gamma} + \mathcal{A}_{\chi_i^\pm}^{\gamma\gamma} \right|^2. \quad (20)$$

The expressions of $\mathcal{A}_i^{\gamma\gamma}$ are relatively simple and are given by

$$\begin{aligned} \mathcal{A}_W^{\gamma\gamma} &= g_{hVV} A_1(\tau_W), \quad \mathcal{A}_t^{\gamma\gamma} = g_{ht\bar{t}} N_c Q_t^2 A_{1/2}(\tau_t), \quad \mathcal{A}_{\tilde{f}_i}^{\gamma\gamma} = \sum_i \frac{g_{h\tilde{f}_i\tilde{f}_i}}{m_{\tilde{f}_i}^2} N_c Q_{\tilde{f}_i}^2 A_0(\tau_{\tilde{f}_i}), \\ \mathcal{A}_{H^\pm}^{\gamma\gamma} &= \frac{m_Z^2 g_{hH^+H^-}}{2M_{H^\pm}^2} A_0(\tau_{H^\pm}), \quad \mathcal{A}_{\chi_i^\pm}^{\gamma\gamma} = \sum_i \frac{2m_W}{m_{\chi_i^\pm}} g_{h\chi_i^+ \chi_i^-} A_{1/2}(\tau_{\chi_i^\pm}), \end{aligned} \quad (21)$$

where $\tau_i = 4m_i^2/m_h^2$, g_{hXY} denotes the Higgs coupling with particles XY and $A_0, A_{1/2}$ and A_1 are loop functions with scalars, fermions and gauge bosons running in the loop. The

explicit expressions of g_{hXY} and A functions are given by

$$g_{hVV} = S_{h1} \sin \beta + S_{h2} \cos \beta, \quad (22)$$

$$g_{ht\bar{t}} = S_{h1} / \sin \beta, \quad (23)$$

$$g_{h\tilde{f}_1\tilde{f}_1} = \frac{-1}{2(\sqrt{2}G_F)^{1/2}} \left(Y_{hLL} \cos^2 \theta_{\tilde{f}} + Y_{hRR} \sin^2 \theta_{\tilde{f}} + Y_{hLR} \sin 2\theta_{\tilde{f}} \right), \quad (24)$$

$$g_{h\tilde{f}_2\tilde{f}_2} = \frac{-1}{2(\sqrt{2}G_F)^{1/2}} \left(Y_{hLL} \sin^2 \theta_{\tilde{f}} + Y_{hRR} \cos^2 \theta_{\tilde{f}} - Y_{hLR} \sin 2\theta_{\tilde{f}} \right), \quad (25)$$

$$\begin{aligned} g_{hH^+H^-} &= \frac{\lambda^2}{\sqrt{2}} \left(v_s(\Pi_{h3}^{11} + \Pi_{h3}^{22}) - v_u\Pi_{h2}^{12} - v_d\Pi_{h1}^{12} \right) + \sqrt{2}\lambda\kappa v_s\Pi_{h3}^{12} + \frac{\lambda}{\sqrt{2}}A_\lambda\Pi_{h3}^{12} \\ &\quad + \frac{g_1^2}{4\sqrt{2}} \left(v_u(\Pi_{h1}^{11} - \Pi_{h1}^{22}) + v_d(\Pi_{h2}^{22} - \Pi_{h2}^{11}) \right) \\ &\quad + \frac{g_2^2}{4\sqrt{2}} \left(v_u(\Pi_{h1}^{11} + \Pi_{h1}^{22} + 2\Pi_{h2}^{12}) + v_d(\Pi_{h2}^{11} + \Pi_{h2}^{22} + 2\Pi_{h1}^{12}) \right), \end{aligned}$$

$$\Pi_{hi}^{jk} = 2S_{hi}C_jC_k, \quad C_1 = \cos \beta, \quad C_2 = \sin \beta,$$

$$v_u = \frac{1}{(\sqrt{2}G_F)^{1/2}}C_2, \quad v_d = \frac{1}{(\sqrt{2}G_F)^{1/2}}C_1, \quad v_s = \mu/\lambda, \quad (26)$$

$$g_{h\chi_i^+\chi_j^-}^L = \frac{1}{\sqrt{2}}(S_{h1}U_{i1}V_{j2} + S_{h2}U_{i2}V_{j1}), \quad g_{h\chi_i^+\chi_j^-}^R = \frac{1}{\sqrt{2}}(S_{h1}U_{j1}V_{i2} + S_{h2}U_{j2}V_{i1}), \quad (27)$$

$$A_0(x) = -x^2 [x^{-1} - f(x^{-1})], \quad (28)$$

$$A_{1/2}(x) = 2x^2 [x^{-1} + (x^{-1} - 1)f(x^{-1})], \quad (29)$$

$$A_1(x) = -x^2 [2x^{-2} + 3x^{-1} + 3(2x^{-1} - 1)f(x^{-1})], \quad (30)$$

where S is the 2×2 (3×3) rotation matrix of MSSM (NMSSM) higgs mass matrix under the basis (H_u^0, H_d^0, S) , h in S_{h1} denotes the row index of the SM-like Higgs, Y_{hXY} denotes the SM-like higgs coupling to sfermion interaction states, U, V denote the rotation matrices of the chargino mass matrix, and $f(x)$ is defined by $f(x) = \arcsin^2 \sqrt{x}$.

As for $A_i^{Z\gamma}$, due to $m_Z \neq 0$ and the existence of ZXY ($X \neq Y$) couplings, their expres-

sions are rather complex

$$\begin{aligned}
\mathcal{A}_W^{Z\gamma} &= g_{hVV} c_w A_1(\tau_W, \lambda_W), \quad \mathcal{A}_t^{Z\gamma} = g_{ht\bar{t}} N_c Q_t \frac{\hat{v}_t}{c_w} A_{1/2}(\tau_t, \lambda_t), \\
\mathcal{A}_{H^\pm}^{Z\gamma} &= -\frac{m_Z^2 g_{hH^+H^-}}{2 m_{H^\pm}^2} v_{H^\pm} A_0(\tau_{H^\pm}, \lambda_{H^\pm}), \\
\mathcal{A}_{\tilde{f}_i}^{Z\gamma} &= -\sum_{\tilde{f}_i} \frac{2 g_{h\tilde{f}_i\tilde{f}_i}}{m_{\tilde{f}_i}^2} N_c Q_{\tilde{f}_i} v_{\tilde{f}_i} A_0(\tau_{\tilde{f}_i}, \lambda_{\tilde{f}_i}) - \mathcal{A}_{\tilde{f}_1\tilde{f}_2}^{Z\gamma}, \\
\mathcal{A}_{\tilde{f}_1\tilde{f}_2}^{Z\gamma} &= \frac{2 g_{h\tilde{f}_1\tilde{f}_2}}{m_{\tilde{f}_1} m_{\tilde{f}_2}} N_c Q_{\tilde{f}} v_{\tilde{f}_2} (A_0^{(1)} + A_0^{(2)}), \\
\mathcal{A}_{\chi_i^\pm}^{Z\gamma} &= \sum_{\chi_i^\pm; m,n=L,R} \frac{2m_W}{m_{\chi_i^\pm}} g_{h\chi_i^+\chi_i^-}^m g_{Z\chi_i^+\chi_i^-}^n A_{1/2}(\tau_{\chi_i^\pm}, \lambda_{\chi_i^\pm}) + \mathcal{A}_{\chi_1^+\chi_2^-}^{Z\gamma}, \\
\mathcal{A}_{\chi_1^+\chi_2^-}^{Z\gamma} &= \frac{2m_W}{\sqrt{m_{\chi_1^\pm} m_{\chi_2^\pm}}} \left((g_{h\chi_1^+\chi_2^-}^L g_{Z\chi_1^+\chi_2^-}^L + g_{h\chi_1^+\chi_2^-}^R g_{Z\chi_1^+\chi_2^-}^R) A_{1/2}^{(1)}, \right. \\
&\quad \left. + (g_{h\chi_1^+\chi_2^-}^L g_{Z\chi_1^+\chi_2^-}^R + g_{h\chi_1^+\chi_2^-}^R g_{Z\chi_1^+\chi_2^-}^L) A_{1/2}^{(2)} \right), \tag{31}
\end{aligned}$$

where $\lambda_i = 4m_i^2/m_Z^2$ and the coupling coefficients of h and Z are given by

$$\hat{v}_t = 2T_3^t - 4Q_t s_w^2, \quad v_{H^\pm} = (c_w^2 - s_w^2)/c_w, \tag{32}$$

$$v_{\tilde{f}_1} = (T_f^3 \cos^2 \theta_{\tilde{f}} - Q_f s_w^2)/c_w, \quad v_{\tilde{f}_2} = (T_f^3 \sin^2 \theta_{\tilde{f}} - Q_f s_w^2)/c_w, \tag{33}$$

$$v_{\tilde{f}_{12}} = (-T_f^3 \sin \theta_{\tilde{f}} \cos \theta_{\tilde{f}})/c_w, \tag{34}$$

$$g_{h\tilde{f}_1\tilde{f}_2} = \frac{-1}{2(\sqrt{2}G_F)^{1/2}} \left(\frac{1}{2} (Y_{hRR} - Y_{hLL}) \sin 2\theta_{\tilde{f}} + Y_{hLR} \cos 2\theta_{\tilde{f}} \right), \tag{35}$$

$$g_{Z\chi_1^+\chi_1^-}^L = (V_{11}^2 + 1 - 2s_w^2)/(2c_w), \quad g_{Z\chi_1^+\chi_1^-}^R = (U_{11}^2 + 1 - 2s_w^2)/(2c_w), \tag{36}$$

$$g_{Z\chi_2^+\chi_2^-}^L = (V_{21}^2 + 1 - 2s_w^2)/(2c_w), \quad g_{Z\chi_2^+\chi_2^-}^R = (U_{21}^2 + 1 - 2s_w^2)/(2c_w), \tag{37}$$

$$g_{Z\chi_1^+\chi_2^-}^L = (V_{11}V_{21})/(2c_w), \quad g_{Z\chi_1^+\chi_2^-}^R = (U_{11}U_{21})/(2c_w). \tag{38}$$

In above formula, we have defined some new functions as

$$\begin{aligned}
A_0^{(1)} &= 4m_{\tilde{f}_1} m_{\tilde{f}_2} (C_{23}^{(1)} + C_{12}^{(1)}) \\
A_0^{(2)} &= 4m_{\tilde{f}_1} m_{\tilde{f}_2} (C_{23}^{(2)} + C_{12}^{(2)}) \\
A_{1/2}^{(1)} &= 2m_{\chi_1^\pm} \sqrt{m_{\chi_1^\pm} m_{\chi_2^\pm}} \left((2C_{23}^{(3)} + 3C_{12}^{(3)} + C_0^{(3)}) + (2C_{23}^{(4)} + C_{12}^{(4)}) \right) \\
A_{1/2}^{(2)} &= 2m_{\chi_2^\pm} \sqrt{m_{\chi_1^\pm} m_{\chi_2^\pm}} \left((2C_{23}^{(4)} + 3C_{12}^{(4)} + C_0^{(4)}) + (2C_{23}^{(3)} + C_{12}^{(3)}) \right) \tag{39}
\end{aligned}$$

with C_{ij} denoting three points loop functions introduced in [65], and $C^{(1)} = C(P_\gamma, P_Z, m_{\tilde{f}_1}, m_{\tilde{f}_1}, m_{\tilde{f}_2})$, $C^{(2)} = C^{(1)}|_{m_{\tilde{f}_1} \leftrightarrow m_{\tilde{f}_2}}$, $C^{(3)} = C^{(1)}|_{m_{\tilde{f}_1} \rightarrow m_{\chi_1^\pm}, m_{\tilde{f}_2} \rightarrow m_{\chi_2^\pm}}$, and $C^{(4)} =$

$C^{(3)}|_{m_{x_1^\pm} \leftrightarrow m_{x_2^\pm}}$. For the special cases considered here, C_{ij} are given by

$$C_0(p_\gamma, p_Z, m_1, m_1, m_2) = - \int_0^1 dy \frac{1}{b} \ln \left| \frac{by + c}{c} \right| \quad (40)$$

$$C_{12}(p_\gamma, p_Z, m_1, m_1, m_2) = \int_0^1 dy \frac{1-y}{b} \ln \left| \frac{by + c}{c} \right| \quad (41)$$

$$C_{23}(p_\gamma, p_Z, m_1, m_1, m_2) = \int_0^1 dy \frac{y(1-y)}{b} \left(1 - \frac{b+c}{by} \ln \left| \frac{by + c}{c} \right| \right) \quad (42)$$

where

$$b = -(m_h^2 - m_Z^2)(1-y), \quad c = -m_Z^2 y(1-y) + m_1^2 y + m_2^2(1-y). \quad (43)$$

Note that for the special case $m_1 = m_2$, these functions can be further simplified to get their analytic expressions. The other functions relevant to our calculation are defined by

$$A_0(x, y) = I_1(x, y), \quad (44)$$

$$A_{1/2}(x, y) = I_1(x, y) - I_2(x, y), \quad (45)$$

$$A_1(x, y) = 4(3 - \tan^2 \theta_w) I_2(x, y) + [(1 + 2x^{-1}) \tan^2 \theta_w - (5 + 2x^{-1})] I_1(x, y), \quad (46)$$

with

$$I_1(x, y) = \frac{xy}{2(x-y)} + \frac{x^2 y^2}{2(x-y)^2} [f(x^{-1}) - f(y^{-1})] + \frac{x^2 y}{(x-y)^2} [g(x^{-1}) - g(y^{-1})], \quad (47)$$

$$I_2(x, y) = -\frac{xy}{2(x-y)} [f(x^{-1}) - f(y^{-1})], \quad (48)$$

$$g(x) = \sqrt{x^{-1} - 1} \arcsin \sqrt{x}. \quad (49)$$

-
- [1] G. Aad *et al.*, [ATLAS Collaboration], Phys. Lett. B **716**, 1 (2012);
- [2] S. Chatrchyan *et al.*, [CMS Collaboration], Phys. Lett. B **716**, 30 (2012).
- [3] G. Aad *et al.*, [ATLAS Collaboration], ATLAS-CONF-2012-162; S. Chatrchyan *et al.*, [CMS Collaboration], CMS-PAS-HIG-12-042, CMS-PAS-HIG-12-043, CMS-PAS-HIG-12-044.
- [4] Y. Gao *et al.*, Phys. Rev. D **81**, 075022 (2010); J. Ellis and D. S. Hwang, JHEP **1209**, 071 (2012).
- [5] M. Carena, I. Low and C. E. M. Wagner, JHEP **1208**, 060 (2012) [arXiv:1206.1082 [hep-ph]].

- [6] A. G.Akeroyd and S. Moretti, Phys. Rev. D **86**, 035015 (2012); A. Kobakhidze, arXiv:1208.5180; M. Carena, S. Gori, I. Low, N. R. Shah and C. E. M. Wagner, arXiv:1211.6136; E. J. Chun *et al.*, JHEP **1211**, 106 (2012); R. Sato *et al.*, Phys. Lett. B **716**, 441 (2012); W. -C. Huang and A. Urbano, arXiv:1212.1399; M. Chala, arXiv:1210.6208; E. O. Iltan, arXiv:1212.5695.
- [7] C. Han, N. Liu, L. Wu, J. M. Yang and Y. Zhang, arXiv:1212.6728 [hep-ph]; I. Picek and B. Radovcic, Phys. Lett. B **719**, 404 (2013) [arXiv:1210.6449 [hep-ph]].
- [8] A. Joglekar *et al.*, arXiv:1207.4235; E. Bertuzzo *et al.*, arXiv:1209.6359; L. G. Almeida *et al.*, JHEP **1211**, 085 (2012); H. Davoudiasl *et al.*, arXiv:1211.3449; B. Batell *et al.*, arXiv:1211.2449; H. M. Lee *et al.*, arXiv:1209.1955; M. B. Voloshin, Phys. Rev. D **86**, 093016 (2012); N. Bonne and G. Moreau, Phys. Lett. B **717**, 409 (2012); S. Dawson and E. Furlan, Phys. Rev. D **86**, 015021 (2012); M. A. Ajaib, I. Gogoladze, Q. Shafi, arXiv:1207.7068; S. Dawson *et al.*, arXiv:1210.6663.
- [9] A. Alves *et al.*, Phys. Rev. D **84**, 115004 (2011); T. Abe, N. Chen and H. -J. He, JHEP **1301**, 082 (2013) [arXiv:1207.4103 [hep-ph]].
- [10] A. Urbano, Phys. Rev. D **87**, 053003 (2013) [arXiv:1208.5782 [hep-ph]].
- [11] M. Carena *et al.* JHEP **1203**, 014 (2012); JHEP **1207**, 175 (2012); U. Ellwanger, JHEP **1203**, 044 (2012); U. Ellwanger, C. Hugonie, arXiv:1203.5048; K. Hagiwara, J. S. Lee, J. Nakamura, JHEP **1210**, 002 (2012); R. Benbrik *et al.*, arXiv:1207.1096; T. Cheng, arXiv:1207.6392; B. Kyae, J.-C. Park, arXiv:1207.3126; H. An, T. Liu, L.-T. Wang, arXiv:1207.2473; J. Ke *et al.*, arXiv:1207.0990; G. Belanger *et al.*, arXiv:1208.4952; N. Liu *et al.*, arXiv:1208.3413; M. Drees, arXiv:1210.6507; S. F. King *et al.*, arXiv:1211.5074; K. Choi *et al.*, arXiv:1211.0875; M. Berg *et al.*, arXiv:1212.5009; L. Aparicio *et al.*, arXiv:1212.4808; C. Balazs, S. K. Gupta, arXiv:1212.1708; K. Cheung, C.-T. Lu, T.-C. Yuan, arXiv:1212.1288; Z. Kang, Y. Liu and G. Ning, arXiv:1301.2204; E. J. Chun and P. Sharma, arXiv:1301.1437.
- [12] J. -J. Cao, Z. -X. Heng, J. M. Yang, Y. -M. Zhang and J. -Y. Zhu, JHEP **1203**, 086 (2012) [arXiv:1202.5821 [hep-ph]].
- [13] A. Drozd *et al.*, arXiv:1211.3580; P. M. Ferreira *et al.*, arXiv:1211.3131; S. Chang *et al.*, arXiv:1210.3439; S. Bar-Shalom *et al.*, arXiv:1208.3195; H. S. Cheon and S. K. Kang, arXiv:1207.1083; A. Arhrib *et al.*, arXiv:1205.5536; J. Chang *et al.*, arXiv:1206.5853; L. Wang and X. -F. Han, Phys. Rev. D **87**, 015015 (2013); N. Chen and H. -J. He, JHEP **1204**, 062

- (2012); B. Swiezewska and M. Krawczyk, arXiv:1212.4100.
- [14] K. Hsieh and C.-P. Yuan, Phys. Rev. D **78**, 053006 (2008); L. Wang and J. M. Yang, Phys. Rev. D **84**, 075024 (2011); J. Reuter and M. Tonini, arXiv:1212.5930; X. -F. Han, *et al.*, arXiv:1301.0090.
- [15] J. S. Gainer, W. -Y. Keung, I. Low and P. Schwaller, Phys. Rev. D **86**, 033010 (2012) [arXiv:1112.1405 [hep-ph]]. S. Y. Choi, M. M. Muhlleitner and P. M. Zerwas, Phys. Lett. B **718**, 1031 (2013) [arXiv:1209.5268 [hep-ph]].
- [16] P. S. Bhupal Dev, D. K. Ghosh, N. Okada and I. Saha, JHEP **1303**, 150 (2013) [Erratum-ibid. **1305**, 049 (2013)] [arXiv:1301.3453 [hep-ph]].
- [17] C. -W. Chiang and K. Yagyu, JHEP **1301**, 026 (2013) [arXiv:1211.2658 [hep-ph]].
- [18] C. -W. Chiang and K. Yagyu, Phys. Rev. D **87**, 033003 (2013) [arXiv:1207.1065 [hep-ph]].
- [19] I. Dorsner, S. Fajfer, A. Greljo and J. F. Kamenik, JHEP **1211**, 130 (2012) [arXiv:1208.1266 [hep-ph]].
- [20] [CMS Collaboration], HIG-12-049-pas; [ATLAS Collaboration], ATLAS-CONF-2013-009.
- [21] Technical Design Report, The ILC Baseline Design, <https://forge.linearcollider.org/dist/20121210-CA-TDR2.pdf>; Technical Design Report, ILC R&D in the Technical Design Phase, <https://forge.linearcollider.org/dist/20121210-CA-TDR1.pdf>.
- [22] G. L. Kane, C. F. Kolda, L. Roszkowski and J. D. Wells, Phys. Rev. D **49**, 6173 (1994) [hep-ph/9312272].
- [23] P. Fayet, Nucl. Phys. B **90** (1975) 104; *ibid.* Phys. Lett. B **64** (1976) 159; *ibid.* Phys. Lett. B **69** (1977) 489; *ibid.* Phys. Lett. B **84** (1979) 416.
- [24] K. Inoue, A. Komatsu and S. Takeshita, Prog. Theor. Phys **68** (1982) 927; (E) *ibid.* **70** (1983) 330.
- [25] U. Ellwanger, C. Hugonie and A. M. Teixeira, Phys. Rept. **496**, 1 (2010) [arXiv:0910.1785 [hep-ph]].
- [26] M. Maniatis, Int. J. Mod. Phys. A **25** (2010) 3505; J. R. Ellis *et al.* Phys. Rev. D **39**, 844 (1989); M. Drees, Int. J. Mod. Phys. A **4**, 3635 (1989); S. F. King, P. L. White, Phys. Rev. D **52**, 4183 (1995); B. Ananthanarayan, P.N. Pandita, Phys. Lett. B **353**, 70 (1995); B. A. Dobrescu, K. T. Matchev, JHEP **0009**, 031 (2000); R. Dermisek, J. F. Gunion, Phys. Rev. Lett. **95**, 041801 (2005); G. Hiller, Phys. Rev. D **70**, 034018 (2004); F. Domingo, U. Ellwanger, JHEP **0712**, 090 (2007); Z. Heng *et al.*, Phys. Rev. D **77**, 095012 (2008); R. N. Hodgkin-

- son, A. Pilaftsis, Phys. Rev. D **76**, 015007 (2007); W. Wang *et al.* Phys. Lett. B **680**, 167 (2009); J. M. Yang, arXiv:1102.4942; U. Ellwanger and C. Hugonie, arXiv:hep-ph/0612133, arXiv:hep-ph/9909260; U. Ellwanger, arXiv:1108.0157.
- [27] J. E. Kim and H. P. Nilles, Phys. Lett. B **138**, 150 (1984).
- [28] A. Djouadi *et al.* [MSSM Working Group Collaboration], hep-ph/9901246.
- [29] A. H. Chamseddine, R. Arnowitt and P. Nath, Phys. Rev. Lett. **49** (1982) 970; R. Barbieri, S. Ferrara and C.A Savoy, Phys. Lett. B **119** (1982) 343; L. Hall, J. Lykken and S. Weinberg, Phys. Rev. D **27** (1983) 2359; N. Ohta, Prog. Theor. Phys. **70** (1983) 542;
- [30] A. Menon, et al., Phys. Rev. D **70**, 035005 (2004); V. Barger, et al., Phys. Lett. B **630**, 85 (2005); C. Balazs, et. al., JHEP **0706**, 066 (2007); C. Panagiotakopoulos, K. Tamvakis, Phys. Lett. B **446**, 224 (1999); Phys. Lett. B **469**, 145 (1999); C. Panagiotakopoulos, A. Pilaftsis Phys. Rev. D **63**, 055003 (2001); A. Dedes, et. al., Phys. Rev. D **63**, 055009 (2001); K. S. Jeong, Y. Shoji and M. Yamaguchi, JHEP **1204**, 022 (2012); JHEP **1209**, 007 (2012).
- [31] U. Ellwanger, G. Espitalier-Noel and C. Hugonie, JHEP **1109**, 105 (2011) [arXiv:1107.2472 [hep-ph]].
- [32] D. J. Miller, R. Nevzorov and P. M. Zerwas, Nucl. Phys. B **681**, 3 (2004) [hep-ph/0304049].
- [33] J. Cao, Z. Heng, J. M. Yang and J. Zhu, JHEP **1210**, 079 (2012) [arXiv:1207.3698 [hep-ph]].
- [34] U. Ellwanger, J. F. Gunion and C. Hugonie, JHEP **0502**, 066 (2005); U. Ellwanger and C. Hugonie, Comput. Phys. Commun. **175**, 290 (2006); G. Degrassi et al., Eur. Phys. J. C **28** (2003) 133.
- [35] J. Cao, H. E. Logan and J. M. Yang, Phys. Rev. D **79**, 091701 (2009) [arXiv:0901.1437 [hep-ph]].
- [36] A. Djouadi, Phys. Rept. **459**, 1 (2008) [hep-ph/0503173].
- [37] C. -S. Chen, C. -Q. Geng, D. Huang and L. -H. Tsai, arXiv:1301.4694 [hep-ph].
- [38] S. Heinemeyer, W. Hollik and G. Weiglein, Eur. Phys. J. C **9** (1999) 343; S. Heinemeyer, W. Hollik and G. Weiglein, Comput. Phys. Commun. **124** (2000) 76; M. Frank et al., JHEP **0702** (2007) 047.
- [39] <http://lepsusy.web.cern.ch/lepsusy/>
- [40] G. Aad *et al.* [ATLAS Collaboration], Phys. Lett. B **718**, 879 (2013) [arXiv:1208.2884 [hep-ex]];
- [41] [CMS Collaboration], CMS-PAS-SUS-12-022.

- [42] U. Ellwanger and C. Hugonie, *Comput. Phys. Commun.* **177**, 399 (2007) [hep-ph/0612134].
- [43] J. Cao, K. -i. Hikasa, W. Wang, J. M. Yang and L. -X. Yu, *JHEP* **1007**, 044 (2010) [arXiv:1005.0761 [hep-ph]].
- [44] G. Bélanger, F. Boudjema, and A. Pukhov, *micrOMEGAs: A Package for Calculation of Dark Matter Properties in Generic Model of Particle Interaction*, ch. 12, pp. 739–790. World Scientific, 2012. http://www.worldscientific.com/doi/pdf/10.1142/9789814390163_0012.
- [45] Dark Attack 2012 Conference Data, <http://dmttools.brown.edu/>
- [46] RAaij *et al.* [LHCb Collaboration], *Phys. Rev. Lett.* **110**, 021801 (2013) [arXiv:1211.2674 [hep-ex]].
- [47] C. Bobeth *et al.*, *Phys. Rev.* **D64**, 074014 (2001); A. J. Buras *et al.*, *Phys. Lett. B* **546**, 96 (2002).
- [48] [The CMS Collaboration], CMS-PAS-HIG-12-051.
- [49] M. Davier *et al.*, *Eur. Phys. J. C* **66**, 1 (2010).
- [50] P. Nath, *Int. J. Mod. Phys. A* **27**, 1230029 (2012) [arXiv:1210.0520 [hep-ph]].
- [51] J. Ellis and K. A. Olive, *Eur. Phys. J. C* **72**, 2005 (2012) [arXiv:1202.3262 [hep-ph]].
- [52] A. Arbey, M. Battaglia, A. Djouadi and F. Mahmoudi, *JHEP* **1209**, 107 (2012) [arXiv:1207.1348 [hep-ph]].
- [53] J. Cao, Z. Heng, D. Li and J. M. Yang, *Phys. Lett. B* **710**, 665 (2012) [arXiv:1112.4391 [hep-ph]].
- [54] G. Aad *et al.*, [ATLAS Collaboration], ATLAS-CONF-2013-034.
- [55] S. Chatrchyan *et al.*, [CMS Collaboration], CMS-PAS-HIG-13-012.
- [56] J. R. Ellis, T. Falk and K. A. Olive, *Phys. Lett. B* **444**, 367 (1998) [hep-ph/9810360].
- [57] J. R. Ellis, T. Falk, K. A. Olive and M. Srednicki, *Astropart. Phys.* **13**, 181 (2000) [Erratum-*ibid.* **15**, 413 (2001)] [hep-ph/9905481].
- [58] P. P. Giardino, K. Kannike, I. Masina, M. Raidal and A. Strumia, arXiv:1303.3570 [hep-ph].
- [59] U. Ellwanger, J. F. Gunion and C. Hugonie, *JHEP* **0507**, 041 (2005) [hep-ph/0503203].
- [60] R. Balest *et al.* [CLEO Collaboration], *Phys. Rev. D* **51**, 2053 (1995);
- [61] J. Cao *et al.*, *JHEP* **1304**, 134 (2013) [arXiv:1301.6437 [hep-ph]].
- [62] Z. Heng, L. Shang and P. Wan, arXiv:1306.0279 [hep-ph].
- [63] [The ATLAS Collaboration], ATLAS-CONF-2013-012.
- [64] [The CMS Collaboration], CMS-PAS-HIG-13-001.

[65] A. Axelrod Nucl. Phys. B **209**, 349 (1982).